

**Magnetic dynamics studies of the newest-generation iron deficiency drugs based on ferumoxytol and iron isomaltoside 1000**

M. Prester, D. Drobac, and Ž. Marohni

Citation: [Journal of Applied Physics](#) **116**, 043910 (2014); doi: 10.1063/1.4891297

View online: <http://dx.doi.org/10.1063/1.4891297>

View Table of Contents: <http://scitation.aip.org/content/aip/journal/jap/116/4?ver=pdfcov>

Published by the [AIP Publishing](#)

---

**Articles you may be interested in**

[Methotrexate conjugated magnetic nanoparticle for targeted drug delivery and thermal therapy](#)

J. Appl. Phys. **115**, 17B516 (2014); 10.1063/1.4866080

[A highly sensitive magnetic biosensor for detection and quantification of anticancer drugs tagged to superparamagnetic nanoparticles](#)

J. Appl. Phys. **115**, 17B503 (2014); 10.1063/1.4862395

[Temperature dependence of magnetic anisotropy constant in iron chalcogenide Fe<sub>3</sub>Se<sub>4</sub>: Excellent agreement with theories](#)

J. Appl. Phys. **112**, 103905 (2012); 10.1063/1.4759352

[Temperature dependence of electron magnetic resonance spectra of iron oxide nanoparticles mineralized in \*Listeria innocua\* protein cages](#)

J. Appl. Phys. **112**, 084701 (2012); 10.1063/1.4757964

[Nanomechanics of magnetically driven cellular endocytosis](#)

Appl. Phys. Lett. **99**, 183701 (2011); 10.1063/1.3656020

---



**AIP** | Journal of Applied Physics

*Journal of Applied Physics* is pleased to announce **André Anders** as its new Editor-in-Chief

# Magnetic dynamics studies of the newest-generation iron deficiency drugs based on ferumoxytol and iron isomaltoside 1000

M. Prester,<sup>a)</sup> D. Drobac, and Ž. Marohić  
*Institute of Physics, P.O.B.304, HR-10 000 Zagreb, Croatia*

(Received 13 June 2014; accepted 15 July 2014; published online 24 July 2014)

Magnetic dynamics studies by AC susceptibility technique have been performed on the two newest-generation iron deficiency drugs, commercialized under the trade names Feraheme and Monofer. In all aspects, these magnetic nanoparticle systems obey a common pattern of superparamagnetism characterized by similar blocking temperatures, average particle sizes, and magnetocrystalline anisotropy energy. However, effective magnetic moments associated with average particle of each drug are remarkably different, being approximately  $10630 \mu_B$  (Feraheme) and  $134 \mu_B$  (Monofer). The difference relies on qualitatively different magnetic interaction permeating the iron cores of the constituent nanoparticles. The nanoparticle of each system can be classified as monodomain ferrimagnet (Feraheme) and almost compensated antiferromagnet (Monofer). In accordance with different associated moments the dipole-dipole interaction between nanoparticles for the two drugs differs for orders of magnitudes but remains safely small at room temperatures. For reference, the corresponding measurements on previously better investigated iron-sucrose haematinic Venofer has been also performed and included in this article. © 2014 AIP Publishing LLC.  
[\[http://dx.doi.org/10.1063/1.4891297\]](http://dx.doi.org/10.1063/1.4891297)

## I. INTRODUCTION

There is explosive growth of applications of magnetic nanoparticles (MNP), particularly in biomedicine.<sup>1,2</sup> One of the fruitful application areas are drugs for treatment of iron deficiency anaemia, available nowadays in increasing number of orally or intravenously administrating preparations.<sup>3</sup> Knowing magnetic properties of these MNP-based drugs, representing a subject of this study, is critically important in their routine characterization. Surprisingly, in spite of rapid progress in applications, there are fundamental issues in understanding magnetism of MNP that are still not resolved as yet. The latter primarily applies to the question of magnetic interactions within bulk and surface of nanoparticles,<sup>4,5</sup> responsible for particles' net effective magnetic moments, as well as to the magnitude and the role of ubiquitous dipole-dipole interactions between nanoparticles. Commercial MNP-based haematinics, produced under stringent synthesis conditions, thus granting high level of reproducibility, represent simultaneously the research samples challenging our understanding of iron-oxide superparamagnetism in general.

On this track, we present in this article our results of the magnetic dynamics studies of the two newest generation haematinics, ferumoxytol (commercial trade name Feraheme<sup>®</sup>—AMAG Pharmaceuticals, USA), and iron isomaltoside 1000 (commercial trade name Monofer<sup>®</sup>—Pharmacosmos, Denmark). Measurements on the drug Venofer<sup>®</sup> (Vifor, Switzerland), characterized by the corresponding magnetic properties published previously,<sup>6</sup> have been also taken for reference. The purpose of this study goes beyond routine characterizations. On the basis of precisely established methodology, presented herewith, we want to scrutinize the

difference between the investigated systems, trying to interpret these differences within general knowledge of superparamagnetism. In this study, we thus show that magnetic interactions within the iron-cores of similar-sized nanoparticles of Feraheme and Monofer samples are qualitatively and quantitatively very different, resulting with the respective effective magnetic moments of the constituent nanoparticles differing in orders of magnitudes. While the latter findings are probably irrelevant for the targeted medical application, they provide interesting clues for interpretation and characterization of magnetic phenomena of MNP systems.

## II. EXPERIMENTAL

Magnetic dynamics was studied by the use of high resolution commercial AC susceptibility system CryoBIND (achieving resolution better than  $2 \times 10^{-9}$  emu, as expressed in the effective magnetic moment). In view of very small signal, generated particularly by Monofer samples, high resolution was critically important in studies presented herewith. Weak measuring AC field of 3.2 Oe (RMS value) has been systematically used in all measurements, taken at several chosen frequencies (7, 77, 231, and 1777 Hz). The measurements have been performed on zero-field-cooled samples in the controlled temperature sweep heating runs at the sweep rate of 1 K/min, typically. Susceptibility measurement by DC SQUID (Quantum Design's MPMS system) has been also performed on Monofer sample. The samples were obtained from pharmacy and prepared for measurements by freeze-drying the liquid content of the vials, followed by pelletizing the dried powder by the use of standard laboratory press. Mass iron concentration in solid samples was measured by ICP-MS (Inductively Coupled Plasma Mass Spectrometry) system (Agilent Technologies 7500cx), and additionally checked

<sup>a)</sup>prester@ifs.hr

by the manufacturer's data on the solution concentration of iron (being 30 mg/ml and 100 mg/ml for Feraheme and Monofer, respectively). The mass iron concentration in the measured solid samples was determined to be 227 mgFe/g (Feraheme) and 228 mgFe/g (Monofer). Quantitative analysis of magnetic dynamics of these two haematinics relies in part on previous knowledge, as specified by the drug's manufacturers and/or published in Refs. 7 and 8. The latter knowledge can be recapitulated as follows:

### A. Ferumoxytol/Feraheme

Feraheme is a non-stoichiometric magnetite ( $\text{Fe}_3\text{O}_4$ )-based nanoparticle system. The constituent particles are coated with polyglucose sorbitol carboxymethylether, formulated with mannitol. The average hydrodynamic diameter is 23.6 nm (as determined by dynamic light scattering). The median diameter of the iron-oxide core of the particles equals 6.2 nm (as determined by TEM). A part of the X-ray spectra ascribed to the crystalline iron-oxide core is consistent with magnetite but there are also lines corresponding to maghemite ( $\gamma\text{-Fe}_2\text{O}_3$ ).

### B. Iron isomaltoside 1000/Monofer

Iron isomaltoside advances a previous formulation, known as iron carboxymaltose. New formulation consists of a special matrix-like structure with interchanging iron-based molecules and linear isomaltoside 1000 oligomers. The average hydrodynamic diameter is 9.9 nm (as determined by dynamic light scattering). The median diameter of the iron-oxide core of the particles equals 6.3 nm (as determined by TEM). Analysis by XRD does not reveal sharp diffraction peaks indicating structures with little crystallinity, being a consequence of small crystal size and structural disorder. The X-ray pattern is closest to the one known to characterize the iron oxyhydroxide akaganeite ( $\beta\text{-FeOOH}$ ).

## III. RESULTS

### A. AC susceptibility measurements

Results of AC susceptibility measurements on Feraheme and Monofer are shown in Figs. 1 and 2. In phase (real) and out-of-phase (imaginary) signals are shown in the main panels and in the insets, respectively. The results are generally consistent with the well-known behavior of superparamagnetic nanoparticles characterized by a frequency-dependent blocking (dynamics-freezing) temperature  $T_b$ : below  $T_b$  both real ( $\chi'$ ) and imaginary ( $\chi''$ ) components of AC susceptibility depend on frequency. Above  $T_b$  the frequency dependence ceases, as well as the imaginary ac susceptibility component, indicating that the relaxation time of the collective (Néel) relaxations of the particles' magnetic moment over the anisotropy barriers becomes marginal on the time scale of the measuring magnetic AC field period. Qualitatively, the results are in full accordance with AC susceptibility measurements on number of other iron-deficiency haematinics.<sup>6</sup> Quantitative differences rely of course on intrinsic magnetic properties among the individual nanoparticle systems. From Figs. 1 and 2, one immediately notes that Feraheme and

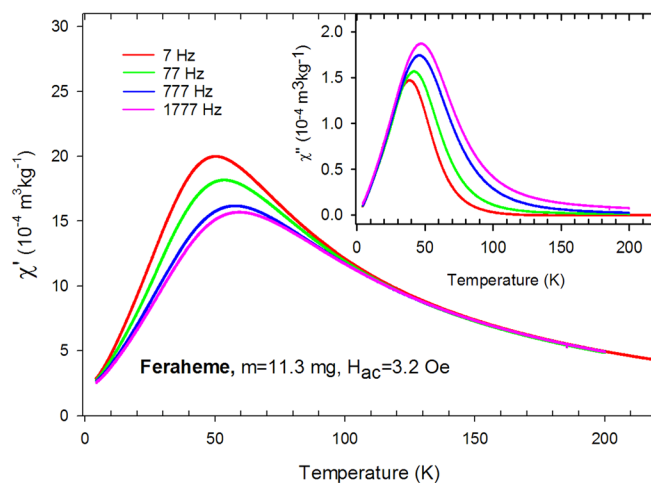


FIG. 1. Results of AC susceptibility measurements on Feraheme sample taken in ac fields at four specified frequencies. Real ( $\chi'$ ) and imaginary ( $\chi''$ ) AC susceptibility components are shown in the main panel and in the inset, respectively.

Monofer mutually differ a lot, first of all in absolute level of susceptibility. Our measurements enable determination of the constant of the effective magnetocrystalline anisotropy energy,  $K_{eff}$ , and the estimation of the effective magnetic moments,  $\mu_{eff}$ , associated with nanoparticles of the two haematinics. The results also enable discussion of the magnetic interactions within the particles. These interactions rule, together with disorder and extrinsic effects, the size of particles' magnetic moments. The results also enable estimations of the residual magnetic interactions between the particles.

### B. Magnetocrystalline anisotropy energy

We determine  $K_{eff}$  for nanoparticle of the average size/volume  $\langle V \rangle$  from the positions  $T_m$  of the maxima in  $\chi''$  in temperature domain: at  $T_m$  dissipation (i.e.,  $\chi''$ ) is maximized at the given field frequency as the applied field period just fits the diverging relaxation time  $\tau$ .  $\tau$  follows the Arrhenius law for magnetic moment of the particle relaxing over the anisotropy energy barrier  $E_a = K_{eff}\langle V \rangle$ ,  $\tau(T) = \tau_0 \exp(E_a/k_B T)$ .

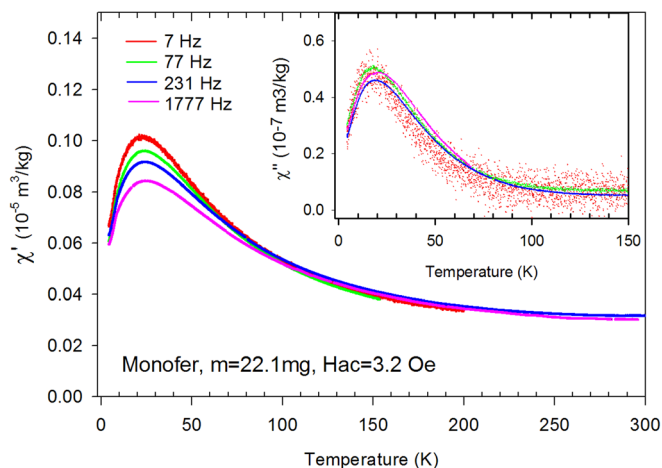


FIG. 2. Results of AC susceptibility measurements on Monofer sample taken in ac fields at four specified frequencies. Main panel: real susceptibility,  $\chi'(T)$ . Inset: imaginary susceptibility,  $\chi''(T)$ .

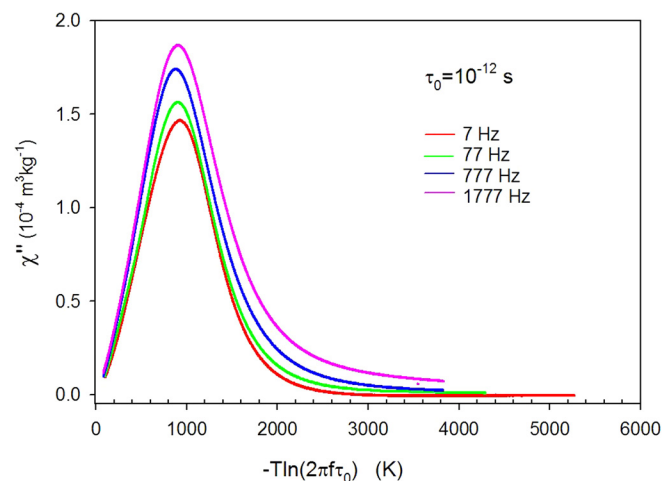


FIG. 3. Results of  $\chi''(T)$  measurements on Feraheme sample after the temperature scale transformation  $T \rightarrow -\ln(2\pi f\tau_0)$  and the search for value of  $\tau_0$  consistent with the best collapse of different curves to a master curve.

Thus,  $K_{eff} = (k_B T / \langle V \rangle) \ln(\tau / \tau_0)$ . The attempt time  $\tau_0$  (the Arrhenius law prefactor) is the time scale for the specific relaxation characterizing the nanoparticle system, revealing weak dependence on many parameters, including temperature and the intensity of the interparticle interactions. It is however justified to treat  $\tau_0$  as a constant in majority of general considerations of magnetic dynamics of various nanoparticle systems. In a widely accepted model for AC susceptibility of magnetic nanoparticles, relying on spin-lattice coupling and quasi-Debye relaxations,<sup>9–11</sup> the temperature dependence of  $\chi''$ , taken at frequency  $f$ , is primarily determined by the distribution of activation energies thus, in view of  $E_a = KV$ , of nanoparticles' volumes.<sup>12</sup> For correct choice of  $\tau_0$ , the transformation of the temperature scale  $T \rightarrow -\ln(2\pi f\tau_0)$  is expected to result with a collapse of all curves taken at different  $f$  on a common master curve.<sup>12</sup> The collapse was indeed identified in  $\chi''(f, T)$  measurements on many magnetic nanoparticle systems, including the iron-deficiency drugs.<sup>6</sup> The usual range for  $\tau_0$ , determined from the temperature scale transformation, is  $10^{-9}$  s –  $10^{-12}$  s; experimental values for  $\tau_0$  found to be much below the latter interval are usually interpreted as a sign of enhanced magnetic interactions between the particles.<sup>6,13</sup> Figs. 3 and 4 show that a collapse of the experimental  $\chi''(f, T)$  curves of Feraheme and Monofer samples takes place for the choice  $\tau_0 \approx 10^{-12}$  s and  $\tau_0 \approx 10^{-13}$  s, respectively. For Feraheme, one also notes that there is a frequency dependence of  $\chi''(f, T)$  maxima—for this reason, there is no real overlap of

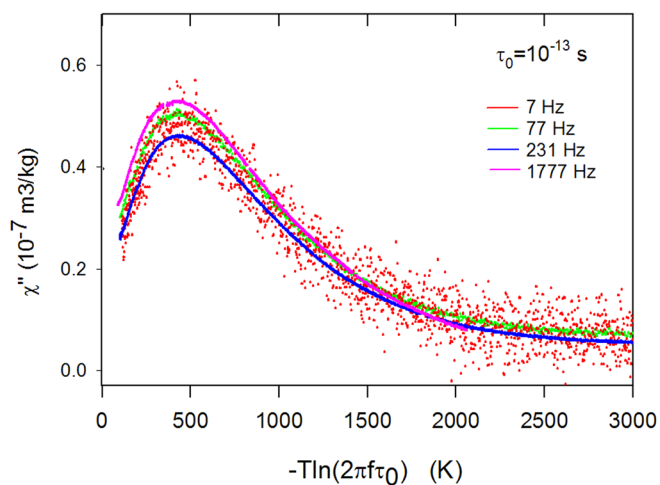


FIG. 4. Results of  $\chi''(T)$  measurements on Monofer sample after the temperature scale transformation  $T \rightarrow -\ln(2\pi f\tau_0)$  and the search for value of  $\tau_0$  consistent with the best collapse of different curves to a master curve.

$\chi''(f, T)$  curves along vertical axis. The latter observation is discussed in Sec. IV.

Upon determination of  $\tau_0$  the effective anisotropy constant  $K_{eff}$  can be calculated for the average-sized particles of the samples, Table I. For comparison, the literature data for the related Venofer samples<sup>6</sup> are also included. All of these values are very close to the typical results referred for ferrihydrite<sup>14</sup> and ferritin<sup>15</sup> nanoparticles of similar average sizes.

### C. Effective magnetic moments

Ideally, in small applied magnetic field  $H$  and at high temperatures (assuring  $k_B T \gg E_d$ ) effective magnetic moments of monodomain nanoparticles  $\mu_{eff}$  performs free rotations ruled by the Zeeman energy  $-\mu_{eff} \cdot H$  and the Boltzmann statistics. The latter (super)paramagnetic regime is then indicated by a Curie-like temperature dependence such that the Curie constant  $C (= \mu_{eff}^2 / 3k_B T)$  enables the most straightforward determination of the particles' mean effective moment. For real systems of magnetic nanoparticles, there are however several reasons why the true Curie regime either does not exist or cannot be easily identified within the experimental temperature- and magnetic field window. The primary cause of the deviation stems from polydispersivity of real samples (distribution of nanoparticle sizes) and the presence of interparticle magnetic interactions.<sup>16</sup> The latter effects result with the transformation of the temperature dependence of initial susceptibility from the

TABLE I. Magnetic parameters of Feraheme (Ferumxtyol), Monofer (Iron Isomaltoside 1000), and Venofer (Iron Sucrose) data, as determined from this magnetic dynamics study. Some previously reported data have been also included.  $\langle D \rangle$  is average particle diameter,  $K_{eff}$  magnetic anisotropy constant,  $n$  the number of Fe ions in average particle,  $\chi_0$  the temperature-independent component of magnetic susceptibility,  $C$  Curie constant (as determined in the high-temperature limit),  $\mu_{eff}^e$  the effective magnetic moment per Fe ion,  $\mu_{eff}$  the effective magnetic moment of the average nanoparticle, and  $T_{d-d}$  the temperature associated with the dipole-dipole interaction.

Sample	Iron core	$\langle D \rangle$ (nm)	$K_{eff}$ ( $10^4$ J/m <sup>3</sup> )	$n$	$\chi_0$ (m <sup>3</sup> /kg)	$C$ (m <sup>3</sup> K/kg)	$\mu_{eff}^e$ ( $\mu_B$ )	$\mu_{eff}$ ( $\mu_B$ )	$T_{d-d}$ (K)
Feraheme	Magnetite	6.2 (Ref. 7)	10.1	5026	$-2.2 \times 10^{-4}$	0.144	150	10630	$3.45 \times 10^{-2}$
Monofer	Akaganeite	6.3 (Ref. 7)	4.4	2867	$-3 \times 10^{-7}$	$4.0 \times 10^{-5}$	2.5	134	$9.54 \times 10^{-6}$
Venofer	Ferrihydrite <sup>21</sup>	5 (Ref. 6)	11.3	1759	$1 \times 10^{-7}$	$1.74 \times 10^{-3}$	16.5	692	$8.6 \times 10^{-5}$

Curie- to the Curie-Weiss form,<sup>16</sup> with the effective “ordering” temperature being a function of the particle size distribution and/or residual interactions.

In determination of the effective magnetic moment, one has to pay special attention to its true origin in antiferromagnetic nanoparticles (like those<sup>6,14,15</sup> that are ferridyhrite- and ferritin-based). Their effective moments rely on imperfect compensation of bulk and/or surface moments of iron ions coupled by strong antiferromagnetic exchange interaction. Unlike ferromagnetic (or ferrimagnetic) particles, revealing big magnetic moments (at the order of  $1000 \mu_B$ , typically) magnetic moment of uncompensated antiferromagnets is much smaller (at the order of  $100 \mu_B$ , typically). Thus, the Zeeman energy of uncompensated moments is proportionally much smaller remaining, in relatively weak applied field, also substantially smaller than the anisotropy energy. The latter energy aligns the uncompensated moments along the randomly positioned easy axes thus the model of “random magnetic orientation”<sup>15</sup> becomes preferable over the standard “free rotation” one (the latter being compatible with the Langevin-type  $M(H)$  dependence). For this reason, the isothermal magnetic field variation  $M(T,H)$  of a nanoparticle systems based on uncompensated antiferromagnets is not well described by the methodology relying on the Langevin function.<sup>15</sup>

Otherwise, fit of the experimental  $M(T,H)$  data to the appropriate model represents a standard route to determine the average effective magnetic moment of the particles. In order to avoid the mentioned uncertainties, permeating the problem of uncompensated antiferromagnets in general, in this work, we present quantitative determination of the effective magnetic moments of the samples on basis of the Curie law only: even in uncompensated magnets, and irrespective of the strength of the anisotropy energy, the Curie law is expected<sup>15</sup> to be strictly obeyed in the low-field limit.

Under the low-field ( $H_{ac} = 3.2$  Oe) conditions of our AC susceptibility measurements the Curie regime characterizes both the Ferumoxytol and the iron Isomaltoside 1000 samples in the high temperature limit, as shown in Figs. 5 and 6.

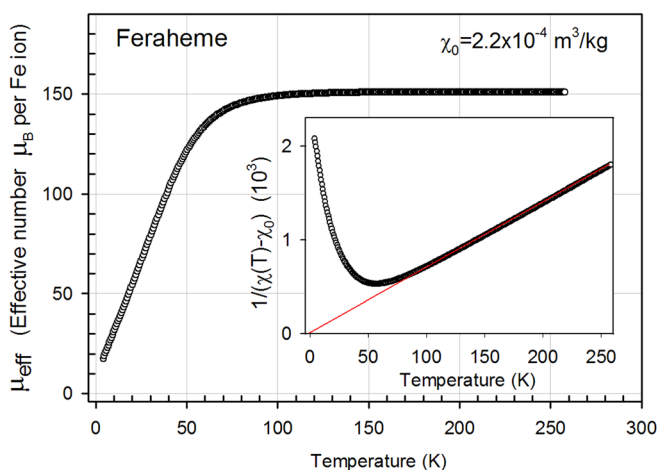


FIG. 5. Main panel: Effective magnetic moment per Fe ion as determined from AC susceptibility measurements on Feraheme sample using Eq. (1). Inset: Inverted data for susceptibility corrected with  $\chi_0$ . The slope in the linear high-temperature range (solid line) is proportional to Curie constant.

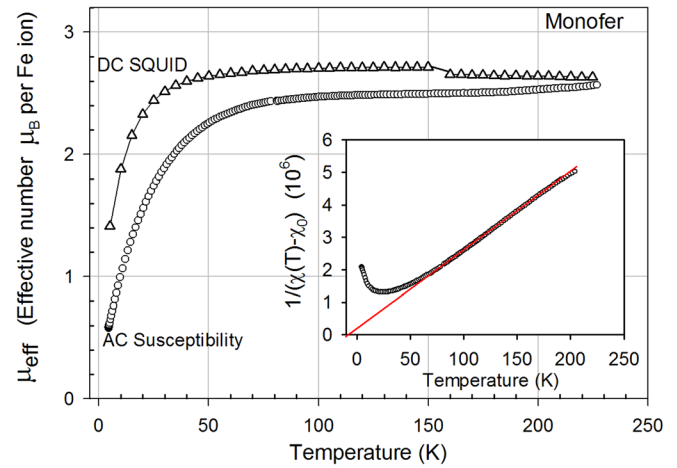


FIG. 6. Main panel: Effective magnetic moment per Fe ion as determined from AC susceptibility measurements on Monofer sample using Eq. (1) (circles). In view of demanding experimental conditions imposed by very weak sample signal DC SQUID susceptibility measurements were also performed in the field of 100 Oe (triangles), for the purpose of additional verification. Obviously, the results for the effective magnetic moment provided by each of the techniques are very similar in the high temperature limit. At low temperatures, the results differ a lot as a consequence of very different frequency window employed by the two techniques. Inset: Inverted data for susceptibility corrected with  $\chi_0$ . The slope in the linear high-temperature range (solid line) is proportional to Curie constant.

For number of other haematinics, the Curie regime has been reported previously.<sup>6</sup> We nevertheless show also the result of our measurement on iron sucrose (Venofer) sample, Fig. 7, playing the role of a reference. The Curie constant  $C$ , determined from these results, enables then the extraction of the average effective magnetic moments characterizing the samples as shown below.

Similarly as in Ref. 6, the Curie constant has been determined by modeling susceptibility  $\chi(T)$  as a sum of the temperature independent component and a component obeying the Curie law,  $\chi = \chi_0 + C/T$ . The Curie constant  $C$  is given by standard expression  $C = \frac{\mu_0}{3k_B} N(\mu_{eff}^{Fe})^2$ , where  $N$  represents

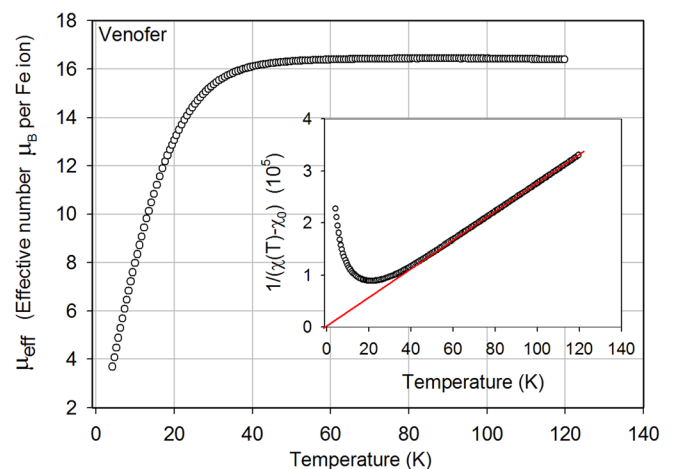


FIG. 7. Main panel: Effective magnetic moment per Fe ion as determined from AC susceptibility measurements on Venofer sample using Eq. (1). In high temperature saturation, the result coincides with the result for Venofer published previously.<sup>6</sup> Inset: Inverted data for susceptibility corrected with  $\chi_0$ . The slope in the linear high-temperature range (solid line) is proportional to Curie constant.

the number of Fe ions per kg and  $\mu_{eff}^{Fe}$  the effective magnetic moment per Fe ion. The temperature independent component  $\chi_0$  is meant to absorb several possible paramagnetic and/or diamagnetic contributions, like a small magnetic contribution of the organic matrix embedding the iron core, the second order-Van Vleck-susceptibility of the magnetic core ions and the parasitic contribution of the sample holder (if any). Additionally, being valid particularly for the uncompensated antiferromagnets, there is also a weakly temperature dependent component of the ordered antiferromagnetic core material<sup>15,17</sup> (relying on canting of the two compensating sublattices). On the basis of previous experimental results on similar systems,<sup>6,15</sup> one can approximate the latter components, due to its smallness, by a constant being included in  $\chi_0$ .

Certainly, a possible incorrectness of any of the latter assumptions would violate a simple Curie-susceptibility form  $\chi = \chi_0 + C/T$ , rendering it meaningless for further interpretation of our results. However, insets to Figs. 5–7 show that the apparent susceptibility of our samples is in fact perfectly compatible with this form. This is even more evident and made quantitative from the main panels of these figures. Instead of a more traditional way of determining  $C$ , from the slope of the  $1/\chi(T)$  plot, we directly show in the main panels the effective magnetic moment per Fe ion  $\mu_{eff}^{Fe}$  by using relationship<sup>18</sup>

$$\begin{aligned}\mu_{eff}^{Fe}(T) &= \left(\frac{3k_B}{\mu_0 N \mu_B}\right)^{1/2} \sqrt{C \times T} \\ &= \left(\frac{3k_B}{\mu_0 N \mu_B}\right)^{1/2} \sqrt{(\chi(T) - \chi_0)T}\end{aligned}\quad (1)$$

commonly used<sup>19</sup> in the evaluations of the effective magnetic moment from the experimental  $\chi(T)$  data.  $\mu_{eff}^{Fe}$  is expressed as the number of Bohr magnetons  $\mu_B$ . Cross-over from the low temperature blocking regime (where  $\mu_{eff}^{Fe}(T)$  has no physical meaning) to the Curie regime at higher temperature is indicated by the  $\mu_{eff}^{Fe}(T)$  function leveling off into the high-temperature saturation, defining also the value of  $\mu_{eff}^{Fe}$  quantitatively.<sup>20</sup>

More than in the effective moment per Fe ion,  $\mu_{eff}^{Fe}$ , one would be interested in the effective moment per nanoparticle,  $\mu_{eff}$ . As there are distribution of particle sizes, thus of the associated magnetic moments, detailed insight into the particle size statistics would in principle be necessary. The latter details are out of scope of this work, focusing primarily the average nanoparticles' data. Thus, we hereby present just the effective moment of the average-size particle. It is related to the measured Curie constant as follows:

$$\begin{aligned}C &= \frac{\mu_0}{3k_B} N (\mu_{eff}^{Fe})^2 = \frac{\mu_0}{3k_B} \sum_p N_p \mu_{eff}^2(p) \\ &= \frac{\mu_0}{3k_B} \int f(V) \mu_{eff}^2(V) dV \approx \frac{\mu_0}{3k_B} N_a \mu_{eff}^2.\end{aligned}\quad (2)$$

Here,  $\mu_{eff}(p)$  represents the effective magnetic moment associated with each in the group of  $N_p$  particles sharing the same volume/moment,  $f(V)$  the particle size distribution

function, and  $N_a$  the equivalent number of average-sized nanoparticles in  $m^3$ , satisfying necessarily  $N(\mu_{eff}^{Fe})^2 = N_a \mu_{eff}^2$ . Taking into account that  $N = N_a n$ , where  $n$  represents the number of Fe ions in the average particle, the latter equality implies<sup>20</sup>  $\mu_{eff}^{Fe} = \mu_{eff}^{Fe} \sqrt{n}$ .

Average effective moment of the particles is determined on basis of the known apparent density of  $Fe_3O_4$ , iron oxyhydroxide akaganeite and ferrihydrite, dominating the crystal structure of Ferumoxytol, iron Isomaltoside 1000, and iron sucrose, respectively.<sup>21,22</sup> The corresponding values<sup>23</sup> are  $5180 \text{ kg/m}^3$ ,  $3640 \text{ kg/m}^3$ , and  $3800 \text{ kg/m}^3$ , respectively. From the average particle sizes characterizing the subject haematinics (Table I) and their molar masses we can then calculate the number of Fe ions  $n$  in the average particle getting finally, from  $\mu_{eff}^{Fe} = \mu_{eff}^{Fe} \sqrt{n}$ , the average moment  $\mu_{eff}$  of the particles.<sup>24</sup> For Feraheme and Monofer, the values of  $\mu_{eff}$  are approximately  $\mu_{eff} = 10630 \mu_B$  and  $\mu_{eff} = 134 \mu_B$ , respectively.

#### D. Dipole-dipole interaction

In view of medical applications of haematinics any residual interaction between the particles that would be responsible for tendency of particle agglomeration cannot be tolerated. A thick organic layer embedding the iron-ion-based particle core eliminates the contribution of exchange interactions thus the only conceivable attractive interaction between the nanoparticles would be a magnetostatic dipole-dipole one. Big effective magnetic moment of the constituent nanoparticles of Feraheme (compared both with the Monofer and Venofer ones, Table I) might indeed cast some doubts whether the strength of dipole-dipole interaction remains reasonably small in this sample at room temperature. The dipole-dipole interaction strength  $E_{d-d}$  can be best estimated from the associated ordering temperature  $T_{d-d}$ ,  $T_{d-d} = E_{d-d}/k_B$

$$T_{d-d} = \frac{\mu_0 \mu_{eff}^2 \mu_B^2}{4\pi k_B d^3} \approx \frac{\mu_0 \mu_{eff}^2 \mu_B^2}{4\pi k_B} N_a, \quad (3)$$

where  $d$  represents the average nanoparticle center-to-center separation, well-approximated by  $d \approx 1/N_a^{1/3}$ , where  $N_a$  represents the number of average-sized nanoparticles in  $m^3$ . From the latter relationship and known sample parameters one finds the average center-to-center separation of the iron-oxide cores to be approximately 127 nm, 105 nm, and 151 nm, for Feraheme, Monofer, and Venofer, respectively. As listed in Table I, the corresponding ordering temperatures for the three haematinics are much below 1K. Due to big effective moment, the dipole-dipole interaction is orders of magnitudes stronger in Feraheme than in the other two nanoparticle systems. However, its very small value of  $T_{d-d} \approx 0.0345 \text{ K}$  demonstrates absence of any conceivable interparticle interaction effect at room temperatures in all three haematinics.

The smallness of the magnetostatic energy  $E_{d-d}$ , on scale of the dominant -activation- energy  $E_a$  implies the decisive quantity for onset of complex dipolar/cluster glass and/or other forms of collective behavior,<sup>25,26</sup>  $E_{d-d}/E_a$ , to be  $E_{d-d}/E_a \ll 1$ . The latter condition, relying first of all on large interparticle separation and achieved by nanoparticles' very architecture, is clearly fulfilled in our samples prepared

and measured in a freeze-dried form. In the manufacturers' original ferrofluid form (packed in glass vials) magnetic dilution is even stronger (inter-particle separation bigger) thus there is no violation of the condition  $E_{d-d}/E_a \ll 1$ . At low temperatures, the liquid-ferrofluid sample freezes (irrespective of the type of solvent) and one expects basically the same type of magnetic dynamics as presented above. At higher temperatures, in the liquid form, one expects a possible contribution of Brown relaxations<sup>1</sup> (dissipative rotations of nanoparticles in viscous medium) to magnetic dynamics. The latter contribution would be maximized at frequencies determined mostly by hydrodynamic properties of the carrier fluid. Identification of the Brownian rotation dynamics in the subject haematinics was out of scope of the present work and was not attempted so far.

#### IV. DISCUSSION AND CONCLUSION

Irrespective from their probably similar biomedical functionalities as iron-deficiency drugs, the two newest generation haematinics, ferumoxytol (Feraheme) and iron isomaltoside 1000 (Monofer), are remarkably different from the point of view of their magnetic structures and low-frequency magnetic dynamics. The main difference relies on the effective magnetic moment of the average constituent nanoparticle being bigger in Feraheme for almost two orders of magnitude. As the physical sizes of average nanoparticles are very similar for the two systems the difference certainly originates from very different exchange interaction Hamiltonians characterizing the two nanoparticle types. While the antiferromagnetic exchange is obviously very efficient compensation mechanism in Monofer (enabling only about  $130 \mu_B$  per average particle) it is significantly less present and efficient in Feraheme (allowing as much as about  $10600 \mu_B$  per average particle). For Feraheme, one also concludes from our experimental data that the related compensation mechanism is strongly particle-size dependent. The latter conclusion follows from the frequency dependence in the magnitude of the imaginary susceptibility peak  $\chi''_M$  (inset to Figs. 1 and 3). The frequency dependent  $\chi''_M$  has otherwise been observed in nanoparticle systems characterized by pronounced dipole-dipole interactions,<sup>26</sup> manifesting an inherently collective magnetism. Interparticle interactions are however vanishingly small in Feraheme thus the frequency-dependent  $\chi''_M$  has to rely on other causes. We claim that the latter frequency dependence represents a direct evidence of non-linear dependence of  $\mu_{eff}$  on  $V$  characterizing the Feraheme nanoparticles. Experimental studies on the system of noninteracting maghemite particles, presented in Ref. 12, can be invoked as an argument. In the latter studies, entirely frequency independent  $\chi''_M$  has been observed and quantitatively reproduced by a model relying on uniform magnetization of the particle volume,<sup>12</sup> i.e.,  $\mu_{eff} \sim V$ . The same model would generate a frequency-dependent of  $\chi''_M$  if one would abandon a simple linear relationship. A closer insight into the specific functional relationship  $\mu_{eff} = f(V)$  valid in Feraheme, relying on precise knowledge of the particle size distribution function, will be subject of a future study.

Finally, it is also relevant to comment potential of the subject pharmaceutical drugs in applications other than iron-deficiency anaemia. Possibility of other applications is especially attractive in view of recent approval of Feraheme and Monofer drugs for use in humans by the respective agencies worldwide (particularly in the United States and/or Europe). In most biomedical applications of magnetic nanoparticles, their effective magnetic moment represents a key parameter, determining functionalities in applications involving both magnetic dynamics and magnetostatic. In view of very small effective magnetic moment of Monofer nanoparticles its use in applications other than iron deficiency anaemia is presently very limited. At variance, very big effective moment characterizing Feraheme enables, in principle, numerous applications. Feraheme is already used as a new contrast agent in MRI diagnostics<sup>8</sup> while the initial studies of functionality of Feraheme in magnetic fluid hyperthermia show promising results<sup>8</sup> as well. On the same track, suitability of Feraheme in nanomagnetic cell actuation and targeting, drug delivery, and cell tracking is reasonable to expect as well.

#### ACKNOWLEDGMENTS

We gratefully acknowledge Dr. K. Zadro for his DC-SQUID measurement, Dr. Vinković Vrček, and Dr. J. Jurasović for analytics of iron by ICP-MS, and Dr. T. Vuletić for freeze-drying of liquid samples. We also acknowledge financing from the projects 035-0352843-2845 of the Croatian Ministry of Science, Education, and Sport.

<sup>1</sup>Q. A. Pankhurst, N. K. T. Thanh, S. K. Jones, and J. Dobson, *J. Phys. D: Appl. Phys.* **42**, 224001 (2009); Q. A. Pankhurst, J. Connolly, S. K. Jones, and J. Dobson, *ibid.* **36**, R167 (2003).

<sup>2</sup>S. A. Majetich, T. Wen, and O. T. Mefford, *MRS Bull.* **38**, 899 (2013).

<sup>3</sup>See <http://www.drugs.com/condition/iron-deficiency-anemia.html> for overview of iron-deficiency drugs.

<sup>4</sup>S. Disch, E. Wetterskog, R. P. Hermann, A. Wiedenmann, U. Vainio, G. Salazar-Alvarez, L. Bergström, and T. Brückel, *New J. Phys.* **14**, 013025 (2012).

<sup>5</sup>N. J. O. Silva, V. S. Amaral, L. D. Carlos, B. Rodríguez-González, L. M. Liz-Marzán, T. S. Berquó, S. K. Banerjee, V. de Z. Bermudez, A. Milan, and F. Palacio, *Phys. Rev. B* **77**, 134426 (2008).

<sup>6</sup>L. Gutiérrez, M. P. Morales, and F. J. Lázaro, *J. Magn. Magn. Mater.* **293**, 69 (2005); L. Gutiérrez and F. J. Lázaro, *ibid.* **316**, 136 (2007).

<sup>7</sup>M. R. Jahn, H. B. Andreasen, S. Fütterer, T. Nawroth, V. Schünemann, U. Kolb, W. Hofmeister, M. Muñoz, K. Bock, M. Meldal, and P. Langguth, *Eur. J. Pharm. Biopharm.* **78**, 480 (2011).

<sup>8</sup>J. P. Bullivant, S. Zhao, B. J. Willenberg, B. Kozissnik, C. D. Batich, and J. Dobson, *Int. J. Mol. Sci.* **14**, 17501–17510 (2013).

<sup>9</sup>A. H. Morrish, *The Physical Principles of Magnetism* (IEEE Press, New York, 2001).

<sup>10</sup>L. Lundgren, P. Svedlindh, and O. Beckman, *J. Magn. Magn. Mater.* **25**, 33 (1981).

<sup>11</sup>M. Prester, I. Živković, D. Drobac, V. Šurića, D. Pajić, and H. Berger, *Phys. Rev. B* **84**, 064441 (2011).

<sup>12</sup>T. Jonsson, J. Mattson, P. Nordblad, and P. Svedlindh, *J. Magn. Magn. Mater.* **168**, 269 (1997).

<sup>13</sup>J. L. Dorman, F. D'Orazio, F. Lucari, E. Tronc, P. Prené, J. P. Jolivel, D. Fiorani, R. Cherkoui, and N. Noguès, *Phys. Rev. B* **53**, 14291 (1996).

<sup>14</sup>N. J. O. Silva, V. S. Amaral, L. D. Carlos, B. Rodríguez-González, L. M. Liz-Marzán, A. Milan, F. Palacio, and V. de Z. Bermudez, *J. Appl. Phys.* **100**, 054301 (2006).

<sup>15</sup>C. Gilles, P. Bonville, K. K. W. Wong, and S. Mann, *Eur. Phys. J. B* **17**, 417 (2000); C. Gilles, P. Bonville, H. Rakoto, J. M. Broto, K. K. W. Wong, and S. Mann, *J. Magn. Magn. Mater.* **241**, 430 (2002).

<sup>16</sup>M. El-Hilo, K. O'Grady, and R. W. Chantrell, *J. Magn. Magn. Mater.* **117**, 21 (1992).

<sup>17</sup>L. Néel, C. R. Acad. Sci. **253**, 9 (1961).

<sup>18</sup>S. Blundell, *Magnetism in Condensed Matter* (Oxford University Press, New York, 2001), p. 195.

<sup>19</sup>S. Hatscher, H. Schilder, H. Lueken, and W. Urland, *Pure Appl. Chem.* **77**, 497 (2005).

<sup>20</sup>The results for  $\mu_{eff}^{Fe}$  and  $\mu_{eff}$  presented in this work should be considered as the first order approximation only. One namely expects, e.g., that there is also a temperature dependence characterizing  $\mu_{eff}$  in reality, as it has been shown for ferridyhrite<sup>14</sup> and ferritin.<sup>15</sup>

<sup>21</sup>Recent article<sup>22</sup> raises some doubts of the crystalline iron core structure of iron sucrose-akaganite structure was favored over the ferrihydrite one in the latter article. We note that the interpretation of our results, e.g., determination of the effective magnetic moment, depends very little of the choice between these two structure as the apparent density of both are very similar (see, main text).

<sup>22</sup>M. Koralewski, M. Pochylski, and J. Gierszewski, *J. Nanopart. Res.* **15**, 1902 (2013).

<sup>23</sup>See [www.webmineral.com](http://www.webmineral.com) for data on apparent density of iron oxides.

<sup>24</sup>Although the form of this relationship suggests the square-root dependence  $\mu_{eff} \sim V^{1/2}$  it does not imply a statement that the effective moment as a whole necessarily depends on particle volume as  $V^{1/2}$ —the prefactor  $\mu_{eff}^{Fe}$  in the relationship involves the volume dependence as well. Thus, we do not discuss in this article the important question<sup>4,5</sup> of the true and intrinsic functional relationship between the effective moment of the particle and its volume.

<sup>25</sup>D. Farrell, Y. Cheng, R. W. McCallum, M. Sachan, and S. A. Majetich, *J. Phys. Chem. B* **109**, 13409 (2005).

<sup>26</sup>C. Djurberg, P. Svedlindh, and P. Nordblad, *Phys. Rev. Lett.* **79**, 5154 (1997).